A model for binaural response properties of inferior colliculus neurons. II. A model with interaural time difference-sensitive excitatory and inhibitory inputs and an adaptation mechanism

Hongmei Cai, Laurel H. Carney, and H. Steven Colburn
Department of Biomedical Engineering, Boston University, 44 Cummington Street, Boston, Massachusetts 02215

(Received 18 November 1996; revised 3 September 1997; accepted 4 September 1997)

The inferior colliculus (IC) model of Cai *et al.* [J. Acoust. Soc. Am. **103**, 475–493 (1998)] simulated the binaural response properties of low-frequency IC neurons in response to various acoustic stimuli. This model, however, failed to simulate the sensitivities of IC neurons to dynamically changing temporal features, such as the sharpened dynamic interaural phase difference (IPD) functions. In this paper, the Cai *et al.* (1998) model is modified such that an adaptation mechanism, viz., an additional channel simulating a calcium-activated, voltage-independent potassium channel which is responsible for afterhyperpolarization, is incorporated in the IC membrane model. Simulations were repeated with this modified model, including the responses to pure tones, binaural beat stimuli, interaural phase-modulated stimuli, binaural clicks, and pairs of binaural clicks. The discharge patterns of the model in response to current injection were also studied and compared with physiological data. It was demonstrated that this model showed all the properties that were simulated by the Cai *et al.* (1998) model. In addition, it showed some properties that were not simulated by that model, such as the sharpened dynamic IPD functions and adapting discharge patterns in response to current injection. © *1998 Acoustical Society of America.* [S0001-4966(98)00601-8]

PACS numbers: 43.64.Bt, 43.66.Pn [RDF]

INTRODUCTION

The inferior colliculus (IC) is a critical structure in the midbrain because it is the target of almost all ascending fibers from the lower auditory brain stem. In recent years, there have been diverse studies of the IC, regarding its morphology and physiology. The physiological responses of low-frequency IC neurons reported in the literature include responses to pure tones (Kuwada and Yin, 1983; Yin and Kuwada, 1983a, b; Kuwada *et al.*, 1984), responses to binaural beat stimuli (Yin and Kuwada, 1983a; Spitzer and Semple, 1991), and responses to interaural phase-modulated tones (Spitzer and Semple, 1993). In addition to the responses to sustained stimuli, the responses of IC neurons to transient stimuli have also been studied, including responses to binaural click stimuli (Carney and Yin, 1989) and to pairs of binaural clicks (Litovsky and Yin, 1993, 1994; Fitzpatrick *et al.*, 1995). All of these studies revealed interesting binaural response properties of the IC. Recently, membrane properties of the IC have been explored by Peruzzi and Oliver (1995) with voltage and current clamping and intracellular recording techniques on slices of the IC from rats. One way to understand these separate data is to build a simple but adequate model which simulates all of the above responses.

There have been several models that simulated the data from the IC, including those of Sujaku *et al.* (1981), Colburn and Ibrahim (1993), Brughera *et al.* (1996), and Cai *et al.* (1998). Among these models, the Cai *et al.* (1998) model was designed to simulate a wide variety of the properties of IC neurons. This model, however, with its membrane equations identical to those of the bushy cell model of Rothman *et al.* (1993), did not describe the sensitivities of IC neurons to dynamically changing temporal features, as represented by nonoverlapping interaural phase difference (IPD) functions in response to interaural phase-modulated (IPM) tones (Spitzer and Semple, 1993) and by sharpened dynamic IPD functions obtained from binaural beat stimuli (Yin and Kuwada, 1983a; Spitzer and Semple, 1991). The mechanism responsible for these phenomena is still not clear; however, it is consistent with an adaptation mechanism. Intracellular recordings from some IC neurons in a slice preparation of the rat midbrain also demonstrated adapting discharge patterns in response to depolarizing current injection (Peruzzi and Oliver, 1995). In this paper, the Cai *et al.* (1998) model is modified by incorporating an adaptation mechanism in the IC model neurons.

The simulation results of this model in response to a variety of stimuli are presented. These stimuli include depolarizing current injection and sustained acoustic stimuli, such as pure tones, binaural beat stimuli, and interaural phase-modulated tones. Although the IC model in Cai *et al.* (1998) successfully described some of these responses, those simulations were repeated with the modified model so that the effects of the adaptation mechanism on these basic responses could be studied. The responses of the model to transient stimuli, including single binaural clicks and pairs of binaural clicks, were also repeated but are not presented in this paper, since the adaptation mechanism did not affect these responses in any obvious way. The responses to transient

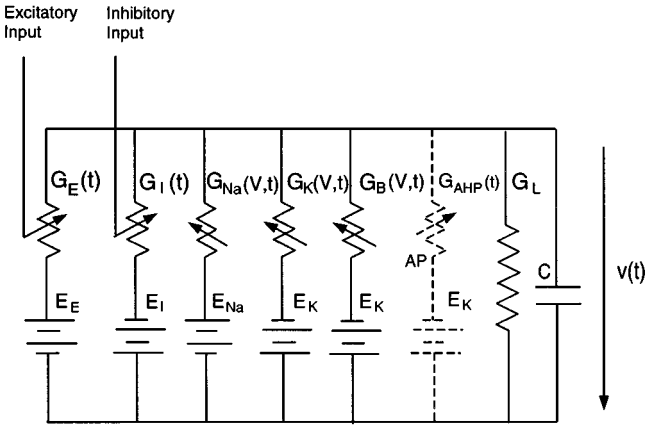

FIG. 1. Circuit diagram of the IC model which was based on the Rothman *et al.* (1993) model but modified with an additional channel simulating a calcium-activated, voltage-independent potassium channel (dashed structure). This channel was triggered by action potentials (APs) in the model.

stimuli were very similar to those obtained with the Cai *et al.* (1998) model (Cai, 1997).

I. METHODS

The structure of the model was identical to the model described in Cai *et al.* (1998). A detailed description of the model structure and each model component is given by Cai *et al.* (1998). The IC model neuron was driven by an ipsilateral medial superior olive (MSO) neuron and inhibited by a contralateral MSO neuron via an inhibitory interneuron, presumed to be within the dorsal nucleus of the lateral lemniscus (DNLL). The MSO model neurons received convergent inputs from model spherical bushy cells (Rothman *et al.*, 1993) which in turn were driven by models of auditory-nerve fibers (Carney, 1993). The model MSO cells might also receive inhibition from onset cells, presumably from globular bushy cells in the anteroventral cochlear nucleus (AVCN). In the following paragraphs, we focus on the difference between the current and the previous model.

The membrane equations for the model IC cell were similar to those of the Rothman *et al.* (1993) model with one modification. An additional potassium channel was added, simulating a calcium-activated, voltage-independent potassium channel which resulted in afterhyperpolarization (AHP) and therefore modulated the discharge frequency. The circuit diagram of the IC model membrane is shown in Fig. 1. The differential equation describing the membrane potential change is

$$C\frac{dV}{dt}+G_B(V-E_K)+G_{\mathrm{K}}(V-E_K)+G_{\mathrm{Na}}(V-E_{\mathrm{Na}})+G_L(V-E_L)+G_I(V-E_I)+G_E(V-E_E)+G_{\mathrm{AHP}}(V-E_K)=I_{\mathrm{ext}}, \quad (1)$$

where C is membrane capacitance. The conductances of the low-threshold, slow potassium channel (G_B), sodium channel (G_{Na}), and delayed-rectifierlike potassium channel (G_{K}) were described by Hodgkin–Huxley-type equations, as given in Rothman *et al.* (1993). The conductance, G_{AHP}, of the channel which leads to the adaptation effects is described in detail below.

Although there is no direct evidence that the calcium-activated, voltage-independent potassium channel exists in the IC, action potentials with a long tail of hyperpolarization have been observed in the intracellular recordings from the IC (Nelson and Erulkar, 1963). In addition, current clamp responses of IC neurons show both regular and adapting discharge patterns (Peruzzi and Oliver, 1995). The adapting pattern could be caused by an AHP mechanism, but other equivalent mechanisms would give similar results.

The conductance of the calcium-activated, voltage-independent potassium channel was modeled in a simplified way. Since the IC model membrane did not have a calcium channel, changes in the conductance of the calcium-activated, voltage-independent potassium channel in the model were triggered by action potentials rather than by an associated calcium influx. The conductance of this channel was increased by a fixed amount half a millisecond after the rising edge of an action potential was detected. Then the conductance decreased exponentially with a long time constant τ_{AHP} (500 ms):

$$G_{\mathrm{AHP}}(t-t_{\mathrm{AP}}-0.5)=G_{\mathrm{AHP}_{\max}}\exp\left(-\frac{t-t_{\mathrm{AP}}-0.5}{\tau_{\mathrm{AHP}}}\right)\times u(t-t_{\mathrm{AP}}-0.5), \quad (2)$$

where t_{AP} is the time when an action potential is detected and the time is measured in milliseconds.

This model was based on the observation that the slow calcium-dependent potassium current followed an exponential function with a time constant of several hundreds of milliseconds in bullfrog sympathetic ganglion cells (Pennefather *et al.*, 1985); however, the exact time course of this current during an action potential is uncertain. In this model, the rapid buildup of internal calcium concentration was simplified by delaying the increment of the AHP conductance by 0.5 ms in our model. This simplification had little effect on the membrane potential both during and after an action potential (Cai, 1997).

Model parameters other than those related to AHP were identical to those used in the IC model of Cai *et al.* (1998).

II. RESULTS

A. Single action potentials

Since the presence of the AHP mechanism changed the differential equation of membrane potentials defined in Rothman *et al.* (1993), it was important to examine the membrane dynamics of the model before the model was used to simulate the responses of IC neurons.

A very short current pulse (1 ms in duration) with sufficient level (200 pA) to trigger an action potential was applied to the model neuron. The current associated with afterhyperpolarization, I_{AHP}, and the membrane potential with and without this current are depicted in Fig. 2(A) and (B), respectively. The amplitude of this current was very small,

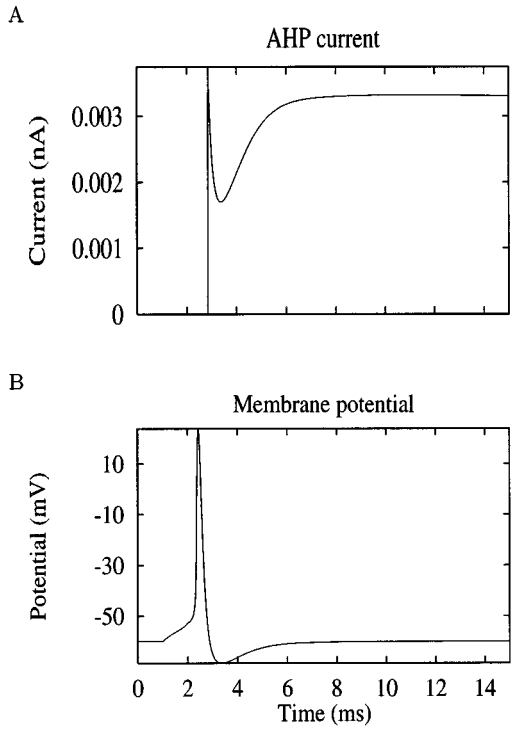

FIG. 2. (A) Current associated with the AHP (I_{AHP}) following the injection of a 1-ms depolarizing current of 200 pA starting at a time of 1 ms. (B) Membrane potentials of the IC models.

thousands of times smaller than those of the sodium current and other potassium currents during an action potential. The extended tail of I_{AHP} (only the initial part is shown) was caused by the slow decay of G_{AHP}, which had a time constant of 500 ms in the model. The model prediction of the current could be compared with the simulation result of another study conducted by Yamada *et al.* (1989). Their model, which was built for bullfrog sympathetic ganglion cells, incorporated sodium and calcium channels, along with three types of potassium channels, including a calcium-activated, voltage-independent potassium channel. In their model, the calculated time constant of I_{AHP} at the peak of internal calcium concentration was 0.5 ms, which was comparable to the 0.5-ms delay followed by the abrupt onset of G_{AHP} in our model. The shape of I_{AHP} in our model resembled Yamada *et al.*'s (1989) model. The dip of I_{AHP} a few milliseconds after the onset in both studies was caused by the hyperpolarization of membrane potential [cf. Fig. 2(B)]. The current increased as the membrane potential returned to its resting potential before a very slow decrease to zero. The time course of membrane activity was slower in the Yamada *et al.* (1989) model, due to its overall different membrane dynamics. Also the rate constants in their model for the bullfrog were normalized for 22 °C, rather than 38 °C as in this study for mammalian neurons.

The action potential generated by the models with AHP is shown in Fig. 2(B). This curve completely overlaps with the action potential generated with the model without AHP. Although I_{AHP} became dominant when other currents returned to zero after an action potential, it was still too small to make any noticeable difference (with current values of model parameters) in the membrane potential compared with that of the model without AHP. Note, however, that a series of action potentials would result in accumulation of calcium (a superposition of I_{AHP} components in our model) so that the membrane potential would eventually be affected by this current.

B. Responses to long-duration current injection

To study the discharge patterns in response to long-duration currents, depolarizing currents with a duration of 250 ms and current levels of 250, 350, and 450 pA were applied to the model. The discharge patterns of the model are shown in the left column panels of Fig. 3. At a low current level (e.g., 200 pA), only one action potential was generated at the onset of current injection (not shown). When the current was 250 pA [Fig. 3(A)], five action potentials were elicited. As the current level was increased, a continuous stream of discharges was generated. Note particularly that the interspike interval of the discharges increased during the current pulse. In the simulation of current injection of 350 pA [Fig. 3(C)], the discharge rate dropped dramatically after 170 ms so that the interspike interval (ISI) did not linearly change with time. At a current level of 450 pA [Fig. 3(E)], the ISI was a linear function of time. The conductance of AHP increased by a certain amount after each action potential. Since the time constant of G_{AHP} was very slow, the conductance accumulated and the threshold of action potentials became larger as a function of time. This increase in threshold in turn meant that a greater depolarization was required to generate an action potential. Therefore the response rate varied with the history of response. This kind of response pattern was referred to as an adapting discharge pattern.

A comparison between the responses of our earlier IC model (Cai *et al.*, 1998) (right column, Fig. 3) and the responses of the current IC model (left column, Fig. 3) showed the effects of AHP mechanism on discharge patterns. A train of equally spaced action potentials was produced for the duration of the current at each current level in the earlier model. At a high current level, the model neuron was depolarized quickly so the response rate was also high. Since the currents associated with each action potential lasted only a few milliseconds, previous action potentials did not affect successive responses. Hence a constant response rate was produced. This kind of response pattern was referred to as a regular discharge pattern.

Notice that the model cell produces multiple action potentials in response to high-level current injection; this result is not consistent with recordings from bushy cells, which respond with action potentials only at the onset of current pulses (Oertel, 1983; Wu and Oertel, 1984), and thus represents a limitation of the model of Rothman *et al.* (1993). However, this sustained response to current injections is not a limitation for modeling many IC neurons. Peruzzi and Oliver (1995) described three response patterns for IC cells: regular and adapting cells had sustained responses to current injection similar to those shown for the model cell (Fig. 3). They also described cells with onset responses to current injection for which the limitations of the Rothman bushy cell

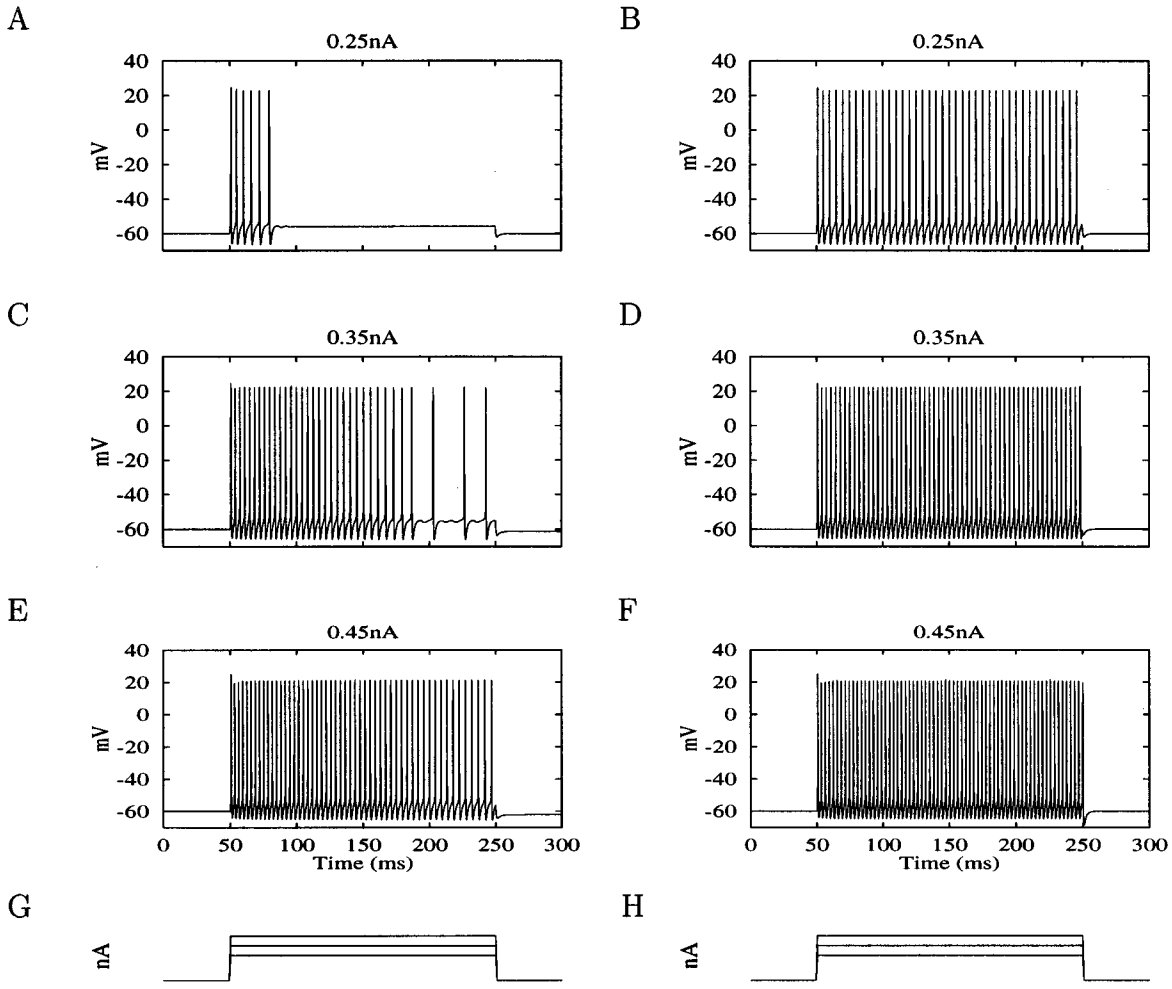

FIG. 3. Discharge patterns of IC models in response to three levels of external depolarizing current. Left column: current IC model. Right column: earlier IC model (Cai *et al.*, 1998). The levels of current are shown on the top of each figure. The current was presented between 50 and 250 ms, as shown in the bottom panels.

model would be a factor; cells with onset responses to current injection were not considered further in this study.

All three types of discharge patterns have been observed in disk-shaped cells and stellate cells of the IC neurons of the rat (Peruzzi and Oliver, 1995). No correlation, however, has been found between the morphology of the neurons and their response types. For the adapting and regular discharge patterns, the interspike interval as a function of time during the current injection could be described as either a linear function or two linear functions crossing each other, depending on the current level (Peruzzi, personal communication). These observations are consistent with the simulation results.

In the following sections, the simulation results of the IC model neuron to acoustic stimuli are presented, including the responses to pure-tone stimuli, binaural beat stimuli, and interaural-phase-modulated stimuli.

C. Responses to pure-tone stimuli

The responses of IC neurons to pure-tone stimuli have been studied extensively by presenting tone stimuli with a delay between the signals to the ipsilateral and contralateral sides. The IPD functions obtained from IC neurons vary in shape [Fig. 3 of Yin and Kuwada (1983a)]. Some of them have a single prominent peak in one phase cycle, while others have more than one peak in a cycle. When the stimulus frequency is changed, the shape of the IPD functions may change (Yin and Kuwada, 1983b). Besides the binaural properties, monaural tone stimuli have also been applied to study the phase locking of the IC neurons (Kuwada *et al.*, 1984). In this section, the ITD sensitivities of IC neurons to tone stimuli at various frequencies and their phase-locking properties were simulated.

1. ITD functions

The pure-tone stimuli in the simulation were 65-dB sine waves with a duration of 3 s. The frequency of the tone was at the characteristic frequency (CF) of the model neuron, which was 500 Hz, unless otherwise indicated. Only one sweep of the stimulus was presented. The response rate for each ITD was calculated from the number of action potentials during the last 2 s of the stimulus. The parameters of the MSO and IC model neurons were identical to those used in the Cai *et al.* (1998) model for corresponding stimuli. The

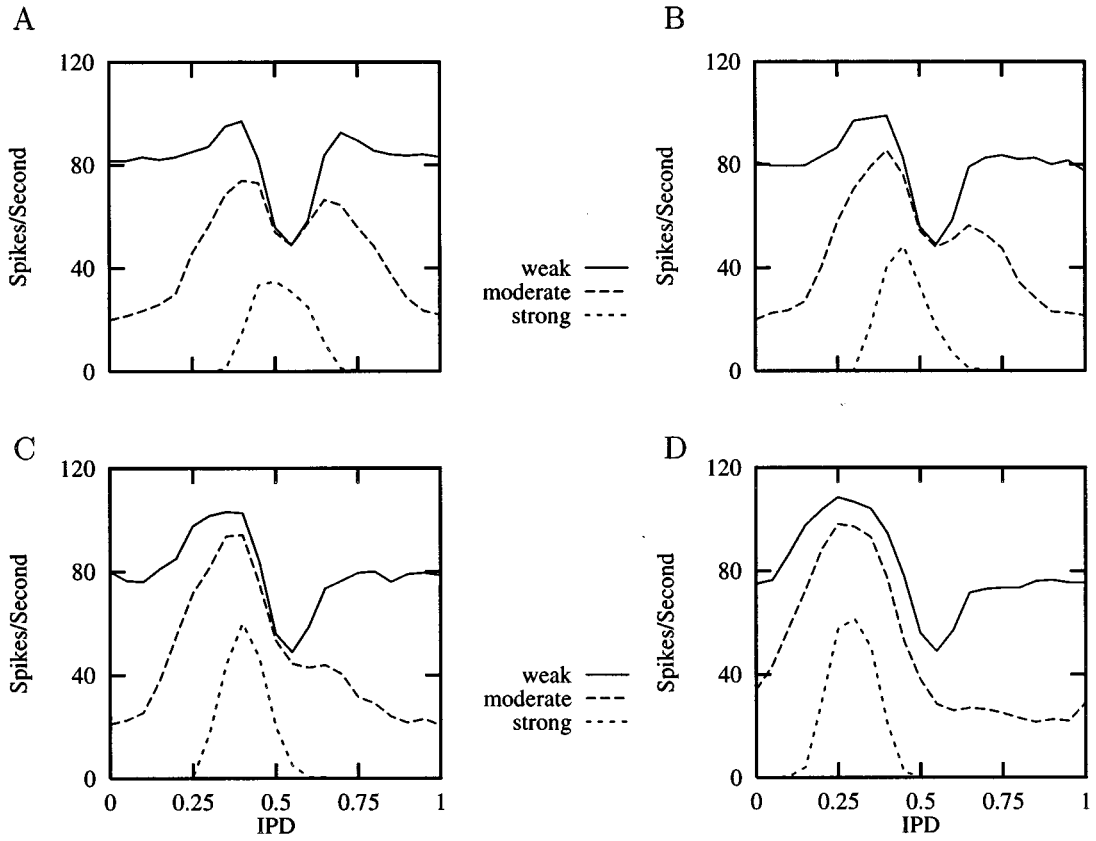

FIG. 4. IPD functions of the IC model neurons when the inhibition to the IC was varied. The CDs of the contralateral MSO model neurons were -60 μs (A), 50 μs (B), 150 μs (C), and 400 μs (D).

inhibitory input parameters to the IC were systematically varied so that three levels of inhibition were obtained: weak, moderate, and strong, as in Cai *et al.* (1998).

The IPD functions of the IC model neurons with four different characteristic delays (CDs) of the contralateral MSO model neuron are shown in Fig. 4. At a high excitatory input rate, the response of the IC saturated at a low rate. Therefore none of the IPD functions followed that of the ipsilateral MSO model neuron, which had a maximum response rate of about 230 spikes/s, even when the inhibition was weak or nonexistent. Both unimodal and bimodal ITD functions were generated with different inhibition levels. Compared with the results from the earlier model (Cai *et al.*, 1998), the overall response rate of these neurons decreased dramatically when the AHP mechanism was incorporated, especially the response rates near the peaks of the IPD function of the ipsilateral MSO model neuron. The basic properties of the IPD functions are consistent with physiological data for both models.

2. Changing stimulus frequency

The ITD functions of the IC model neurons at three frequencies, 400, 500, and 600 Hz, were generated. The stimulus intensity and duration were the same as those in previous simulations. Figure 5 shows the ITD functions of the ipsilateral MSO and IC model neurons (with the CD of the contralateral MSO model neuron at 50 μs) at the three frequencies. These IC model neurons are the same as those of which the responses are shown in Fig. 4(B). The ITD functions of the ipsilateral MSO model neuron [Fig. 5(A)] were sinusoidlike functions with a frequency equal to the stimulus frequency. By visual inspection, these functions showed a common peak at the CD of the model neuron, which was 100 μs, and the relationship between the mean interaural phase of the response and the stimulus frequency is linear. The ITD functions of the IC model neurons, however, did not show a common peak at a certain ITD [Fig. 5(B), (C), and (D)]. None of the ITD functions of these IC model neurons followed that of the ipsilateral MSO model neuron because of both the adaptation mechanism and the inhibition from the contralateral MSO model neuron. For an IC model neuron with only excitation from an ipsilateral MSO model neuron with a low response rate, such that the response of the IC model neuron was not saturated, the peaks of ITD functions at different frequencies would be at the same ITD, as in the MSO model neurons.

3. Phase locking to monaural stimuli

The phase locking of the IC model neurons was studied in the same way as the earlier model (Cai *et al.*, 1998). A monoaural tone of 500 Hz was used in the simulation. Figure 6 shows the mean synchronization index of the ipsilateral MSO model neuron and IC model neurons with weak, moderate, and strong inhibition. The CD of the ipsilateral MSO was 100 μs and that of the contralateral MSO was 50 μs. Two values of the excitatory synaptic strength were studied, i.e., 25 and 16 nS. The synchronization index of the IC

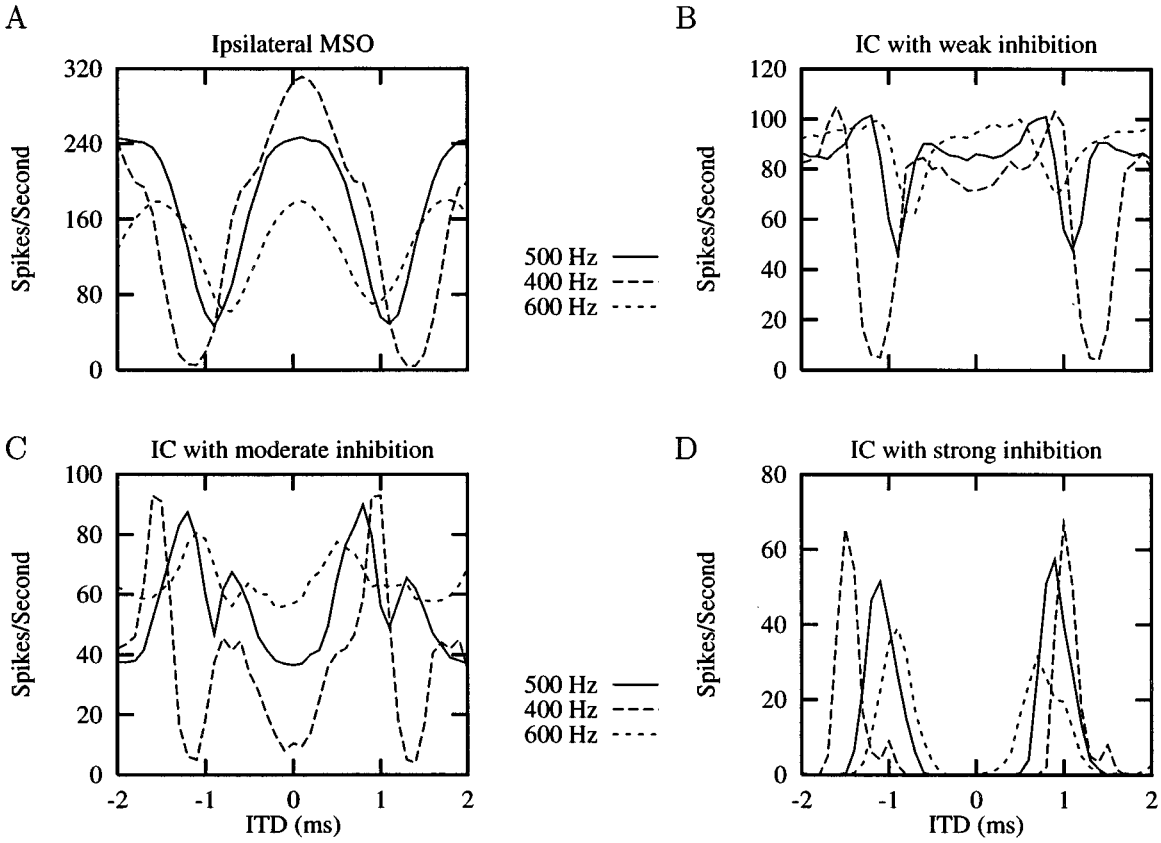

FIG. 5. ITD functions of ipsilateral MSO and IC model neurons at different frequencies.

model neuron with strong inhibition and excitatory synaptic strength of 16 nS was not plotted, because the calculated index did not pass the Rayleigh test (Cai *et al.*, 1998; Mardia, 1972). It can be seen that in both cases, the synchronization indices of the IC model neurons were slightly lower than those of the ipsilateral MSO model neuron. The synchronization index decreased as the inhibition became stronger. The decrease of phase locking was greater in the case of 16 nS, when the relative inhibition was stronger.

The membrane potential was also influenced by the history of the response of the neuron. The variation in membrane potential affected the time of firing and thus the phase locking. In this case, both inhibition to the IC and the adaptation mechanism contributed to the decrease of phase locking. Therefore the synchronization index was lower in the model with AHP than in the model without AHP (Cai *et al.*, 1998). In neither case, however, was the decrease of phase locking in the IC model neurons with respect to MSO model neurons comparable with that observed in physiological data.

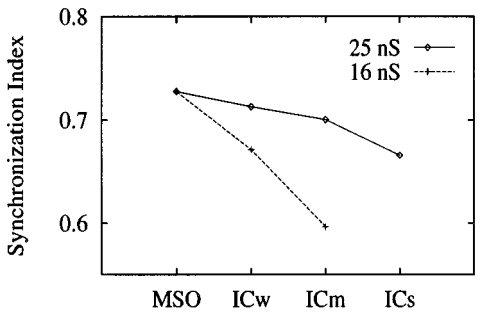

FIG. 6. Synchronization index of ipsilateral MSO and IC model neurons. The excitatory synaptic strengths were 25 and 16 nS. The IC model neurons with weak, moderate, and strong inhibition are represented by ICw, ICm, and ICs, respectively. The synchronization index of ICs at 16 nS is not shown due to the failure of the Rayleigh test (Cai *et al.*, 1998; Mardia, 1972). The CD of the ipsilateral MSO was 100 μs, whereas that of the contralateral MSO was 50 μs. The synchronization index was the average of those obtained from monaural stimuli of the two sides. Stimulus was a 500-Hz monaural tone with a duration of 3 s.

D. Responses to binaural beat stimuli

The binaural beat stimulus in this study consisted of two tones presented to the two sides of the model, one at 500 Hz and the other at 501 Hz, unless otherwise indicated. The IPD functions obtained from binaural beat stimuli were referred to as dynamic IPD functions, whereas those obtained from pure tones were referred to as static IPD functions.

1. Comparison of dynamic and static IPD functions

The comparisons of dynamic and static IPD functions of IC neurons can be found directly or indirectly in the literature. Normalized dynamic and static IPD functions were given in Yin and Kuwada (1983a, their Fig. 3). The dynamic functions appear sharper than the static ones in that the amplitude differences between peaks and troughs are usually larger in the dynamic functions. For one neuron, both the peristimulus time (PST) histogram of responses to binaural beat stimulus and the ITD function of tone responses are given [Fig. 2 of Yin and Kuwada, (1983a)], the absolute (not normalized) response

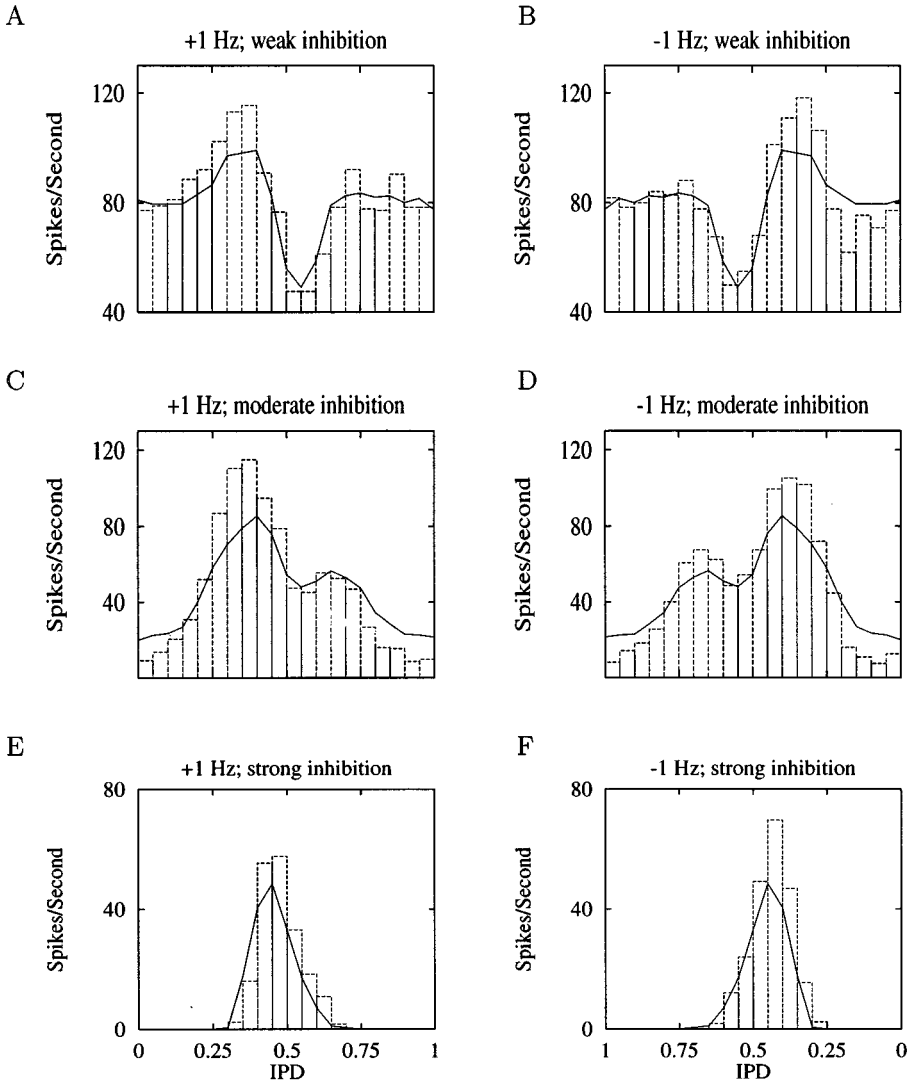

FIG. 7. Dynamic IPD functions (bars) of IC model neurons obtained from binaural beat stimulus along with the static IPD functions (solid curves) obtained from tone stimulus. The beat frequency and the inhibition level to the IC are indicated on the top of each panel.

rates of the dynamic IPD function could be calculated and compared with the static function. Results show that the peak response rate obtained from the binaural beat stimulus (about 96 spikes/s) is much larger than that obtained from the tone stimulus (about 75 spikes/s). A more direct comparison of the dynamic and static IPD functions was provided by Spitzer and Semple (1991), who showed results in an IC cell for which the peak of the dynamic function was twice as high as that of the static function.

The dynamic IPD functions of the IC model neurons with weak, moderate, and strong inhibitions are shown in Fig. 7. Consistent with physiological data, the dynamic IPD functions had the same general shape as the static ones; however, the exact response rates were different between the two functions. The dynamic functions were sharper than the static functions, as observed in real IC neurons (Yin and Kuwada, 1983a; Spitzer and Semple, 1991). At the peak of the IPD function, the response to the dynamic-IPD stimulus was higher than that to the static one. At the trough of the function, the opposite was true. For a given IPD, the difference in the stimuli was the history of temporal features. For tone stimuli, the IPD was kept constant during the entire stimulus duration, while for binaural beat stimuli, the IPD changed with time. The model neuron tended to respond less strongly if it had responded strongly in its recent history (which could be hundreds of milliseconds or even seconds). The adaptation mechanism enabled the model neuron to ''remember'' the history or context of its responses.

2. Rate and direction sensitivities

Some IC neurons are sensitive to the direction and/or the speed of binaural beat stimuli (Yin and Kuwada, 1983a). The responses of such neurons were modeled by choosing different input parameters for the IC model neuron. Figure 8 shows the responses of the model neuron, which had the same parameters as the one in Cai *et al.* (1998) which showed rate and direction sensitivities. This model neuron responded strongly at a lower beat rate and negative beat frequency. In this model, the long-lasting inhibitory effect was still the key for direction and rate sensitivities. The adaptation mechanism did not have much effect on these sen-

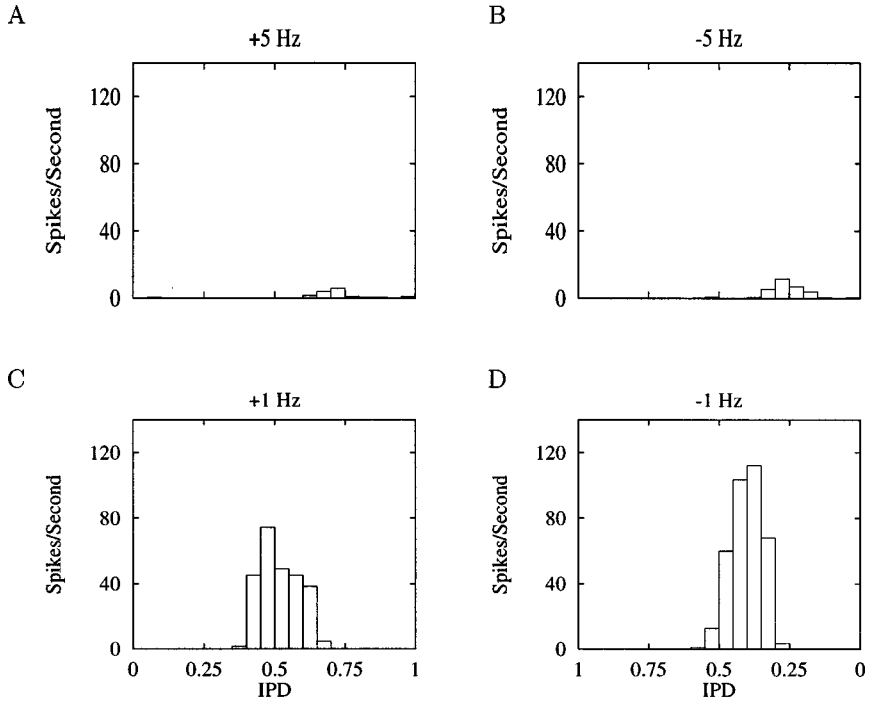

FIG. 8. IPD functions of a direction- and rate-sensitive IC model neuron. The neuron responded more vigorously when the rate of the binaural beat was slow and when the direction of the beat was towards the ipsilateral ear (-1-Hz beat frequency).

sitivities of the IC model, except for small effects on the overall response rate at a beat frequency of ± 1 Hz. This model shows some of the properties observed in the physiological data, but not all (cf. Cai *et al.*, 1998).

E. Responses to interaural phase-modulated (IPM) stimuli

The IPM stimulus is different from the binaural beat stimulus in the extent of the phase variation. For the binaural beat stimulus, the IPD in each beat cycle spans a fixed range of 360°, while in the IPM stimulus, both the range and the mean of the IPD could be varied.

The effect of context or history on IPD-tuning properties was examined by comparing the responses over equivalent ranges of IPD presented within the context of different dynamic stimuli (Spitzer and Semple, 1993, reprinted in Fig. 9). It was found that the IPD functions in each partially overlapping IPD range were nonoverlapping. When compared with the static IPD function obtained from tone stimuli, these functions often showed an ''overshoot'' (at the rising edge) or ''undershoot'' (at the falling edge). These data could not be described by our earlier model (Cai *et al.*, 1998).

In the simulation, the interaural phase disparity was a triangular waveform with a constant offset, as it was in Spitzer and Semple (1993). The carrier frequency of both tones was set at the CF of the model neuron (500 Hz). The modulation frequency was 2 Hz with a modulation depth of 90° at various phase offsets. These parameters were chosen such that the IPD changed at the same speed as in the simulations of binaural beat stimuli and as that used in physiological experiments (Spitzer and Semple, 1993), which was 360°/s. A sequence of stimuli was presented with phase offset from 45° to 315°, with a step of 45°. Since the step of phase offset equals one-half of the modulation depth (90°), the IPD ranges shared one-half of the entire modulation depth with adjacent stimuli.

The duration of the stimulus was 10 s, and it was repeated four times. The PST histograms of the last 9 s were averaged and converted to an IPD function. The IC model input parameters were identical to those used in the simulation of responses to binaural beat stimuli and to those used in Cai *et al.* (1998) for the simulation of the same responses, except for the addition of the AHP-related conductance.

To compare the responses to overlapping IPD regions, profiles of the individual period histograms are plotted on a common IPD axis. Figure 10 shows the IPD sensitivities of three model neurons, with ''weak,'' ''moderate,'' and

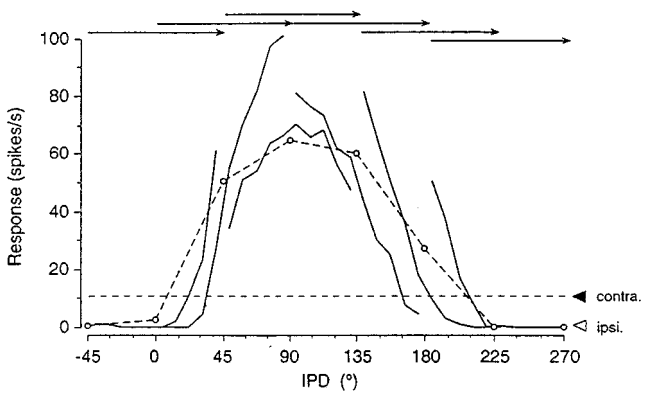

FIG. 9. IPD functions (solid curves) of an IC neuron in response to IPM stimuli, along with the static IPD function (dashed curve). [From Fig. 7 of Spitzer and Semple (1993) reprinted with permission.]

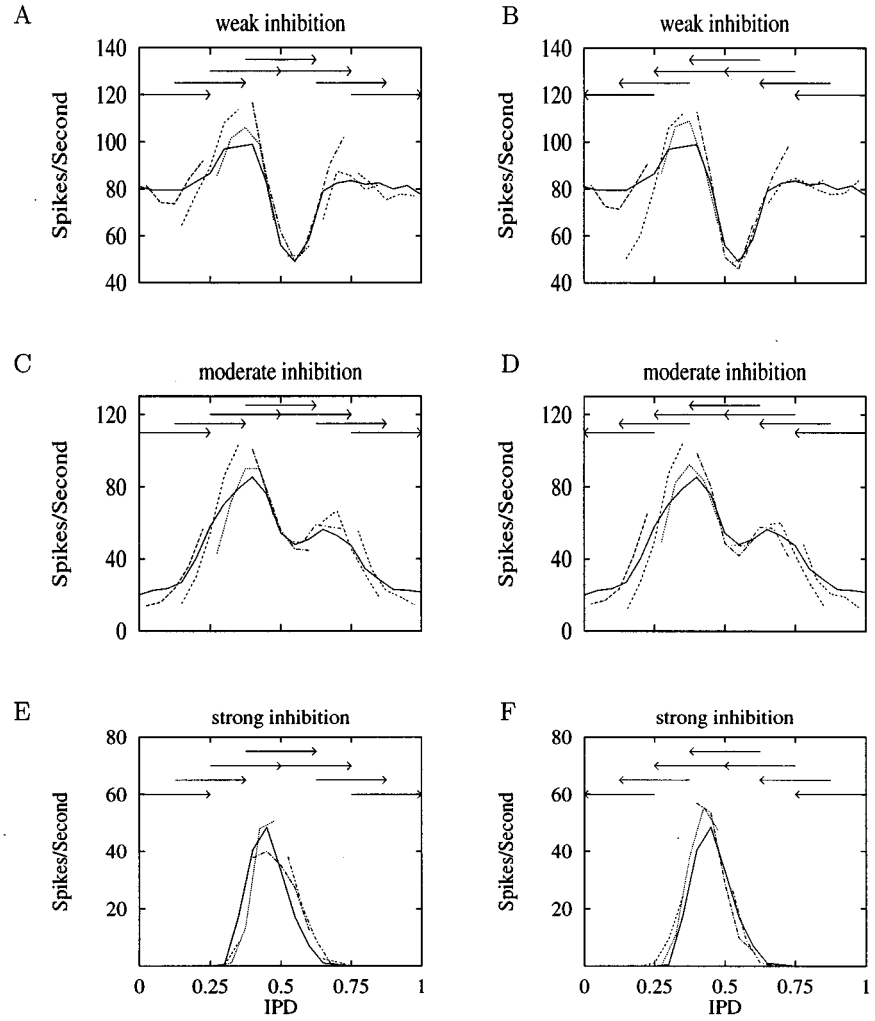

FIG. 10. IPD functions of three model neurons with ''weak inhibition'' [(A) and (B)], ''moderate inhibition'' [(C) and (D)], and ''strong inhibition'' [(E) and (F)], obtained from IPM stimuli (dashed curves). The solid curves are the static IPD functions obtained from a 3-s tone. Arrows on the top show the range and direction of IPD change in IPM stimuli. The rate of IPD change was 360°/s.

''strong'' inhibition, in response to IPM stimuli (dashed curves), along with their static IPD functions (solid curves). Curves on the left column correspond to increasing IPD, while those on the right correspond to decreasing IPD. It can be seen that the profiles of IPD in response to IPM stimuli did not overlap with each other, although the trend of the group of profiles followed the general shape of the static IPD function. The discharge rate at any given IPD depended on the recent history of the stimulus. A systematic relation between the discharge rate in IPM and in static IPD exists such that the dynamic IPD arcs were always steeper than the static IPD function, no matter which direction the IPD changed. If the profiles for the two directions (left-hand panel and right-hand panel) of a neuron were plotted together, they would not be identical. This result is not surprising since the recent history was different for IPD changes in opposite directions. The same phenomenon has been observed in physiological data (Spitzer and Semple, 1993, Fig. 9).

The degree of discontinuity between the static IPD function and dynamic IPD profiles varied over the IPD range (from zero to unity). For example, from panels (A) and (B) of Fig. 10, it seems that the difference between dynamic IPD profiles and the static IPD function near an IPD of 0.55 (the trough of the curve) was not so apparent as those elsewhere. Since the slope near the trough of the static IPD function was sharper than anywhere else on the curve, the impact of changing IPD was not as obvious. Thus there was a limit of maximum response-rate change for a given set of parameters of the IC model. When the rate change or slope approached this limit, the effect of dynamic temporal features was not apparent.

Although the majority of neurons (more than 90%) is sensitive to dynamic stimulus features, the sensitivity varied among these units (Spitzer and Semple, 1993). The three model neurons in Fig. 10 also showed different sensitivity to temporal stimulus features. The one with ''strong inhibition'' [Fig. 10(E) and (F)] was the most insensitive neuron of the three. The low overall response rate and sharp IPD tuning were the causes of the relative insensitivity. Different AHP parameters, e.g., the time constant and conductance increment, might also result in different sensitivities for dynamic

IPD variation. Variations in these parameter values were not explored.

III. DISCUSSION

Simulation results demonstrated that the IC model with an adaptation mechanism was able to simulate diverse physiological data of the IC, including the responses of IC neurons to depolarizing current injection, pure tones, binaural beat stimuli, and interaural phase-modulated tones. In particular, this model was able to simulate response properties that were not described by the IC model without the adaptation mechanism (Cai *et al.*, 1998), including the adapting discharge patterns in response to current injection and the sensitivities to dynamic temporal features.

Based on the physiological model in Cai *et al.* (1998), a single channel added to the membrane equation is adequate in describing these features of the IC. If a generic model were used, the modification might be more complicated and less physiologically interpretable.

A. Adaptation in the IC

Although the sensitivity of IC neurons to interaural delay has been studied in detail, both with tone stimuli and binaural beat stimuli, the difference between the static and dynamic IPD functions has received little attention. The adaptation of IC neurons as reflected in the response rate has been observed not only in the binaural responses, but also in monaural responses. For example, neuron 78197-5 in Kuwada *et al.* (1984) showed a slow adaptation in response to a 1-s tone applied to the contralateral ear.

A model for an IC neuron that included an afterhyperpolarization current (I_{AHP}), simulating a calcium-activated, voltage-independent potassium current, was able to show the adaptation observed in physiological data. The I_{AHP} has been found in many sites of the nervous system in different species, e.g., bullfrog sympathetic neurons (Pennefather *et al.*, 1985), hippocampal pyramidal neurons (Sah and Isaacson, 1995), rat skeletal muscle (Romey and Lazdunski, 1984; Blatz and Magleby, 1986), neuroblasma cells (Hugues *et al.*, 1982) and vagal motoneurons in the guinea pig (Sah, 1995). However, it is not known whether a calcium-activated, voltage-independent potassium channel exists in the IC. The afterhyperpolarization, which has been observed in the intracellular recordings of the IC (Nelson and Erulkar, 1963), could also be explained by a slow inhibitory postsynaptic potential. If this were true, then there would be three candidates for the inhibitory inputs to the IC.

First, intrinsic inhibitory circuitry might exist within the IC. Immunocytochemistry studies demonstrated that up to 20% of the neurons in the central nucleus of the IC are GAD- or GABA-positive (Oliver *et al.*, 1994). Since most, if not all, of the neurons in the IC contribute local axonal collaterals (Oliver and Morest, 1984; Oliver *et al.*, 1994), the GABAergic neurons in the IC are expected to contribute to local inhibitory synapses. Many GABA-positive neurons are large or medium sized. Some of them have processes oriented in parallel with the fibrodendritic laminae; therefore, these neurons may be disk-shaped cells with axons confined to the lamina of origin. Hence it is possible that they provide a delayed suppression to other neurons with similar CF.

Second, the input might come from the corticofugal pathway. Anatomical studies have demonstrated cortico-thalamic, cortico-collicular, and colliculo-olivary efferent pathways. Recent tract-tracing studies in the cat have demonstrated descending projections from the auditory cortex to all subdivisions of the IC, including the central nucleus (Feliciano and Thompson, 1995). It was shown that electrical stimulation of the primary auditory cortex (AI) inhibited the acoustically evoked responses of neurons in the inferior colliculus in bats (Sun *et al.*, 1989). Electrical stimulation of the AI of the cat also generated excitatory postsynaptic potentials (EPSPs), inhibitory postsynaptic potentials (IPSPs), or EPSP-IPSP sequences in IC neurons (Mitani *et al.*, 1983).

Third, the inhibitory input from the ascending pathway, e.g., from DNLL, is a possible source. The GABAergic synapse from the DNLL contributes to one third of the GABAergic synapses in the IC (Shneiderman *et al.*, 1988).

The responses of the inhibitory input to the IC must be highly correlated with those of the neuron to which it is projecting. Otherwise, the dynamic responses may not follow a consistent rule when compared with the static IPD sensitivity. If the two neurons are highly correlated, a simple neural circuit to implement this function would have the IC neuron send inhibition to itself with a short delay simulating the neural transmission time. This recurrent inhibition can be modeled in exactly the same way as the AHP in the simulation presented in this study, except that the reversal potential of the channel associated with the AHP may not be the potassium equilibrium potential. The simulation result should be similar to that obtained in this study.

It is important to note that this inhibition cannot replace the inhibition from the contralateral MSO in the model. This inhibition cannot explain the ITD-dependent echo suppression observed in the IC, since internal inhibition linked to the cell would allow only the leading stimulus with an ITD that evokes a strong response to be more suppressive. Although no data are available on both the ITD dependence of echo suppression and IPM response from a single IC neuron, it is unlikely that the adaptation and echo suppression originate from the same source. The former is much weaker than the latter. The neural mechanism that causes dynamic sensitivity requires further study.

There are several other ways of creating neural modulation, including changes in the amount of neurotransmitters released at presynaptic sites; changes in the synthesis, transport, and processing of neurotransmitters; and changes in the conductances of ion channels of the membrane. It is unlikely that the neural modulation (or adaptation) in the IC is completely caused by these factors, since adaptation was observed with the injection of depolarizing currents (Peruzzi and Oliver, 1995), which were not related to neurotransmitters. The postsynaptic adaptation mechanisms include prespike (e.g., M current) and postspike (e.g., AHP current) mechanisms. The M current is activated at a membrane potential between the resting potential and the threshold of action potential, whereas the AHP current is activated by calcium influx during an action potential. These two

TABLE I. Summary of the abilities of MSO (Brughera *et al.*, 1996), IC model without adaptation (Cai *et al.*, 1998), and IC model with adaptation as described in this paper. ''√'' indicates that the model can describe the property of data. ''×'' indicates that it cannot.

Properties	MSO	IC without adaptation	IC with adaptation
Unimodal ITD functions	√	√	√
Early or late inhibitions	√	√	√
Bimodal ITD functions	×	√	√
Direction and rate sensitivity	×	√	√
ITD-dependent echo suppression	×	√	√
Sharpened dynamic IPD functions	×	×	√
Adapting discharge pattern	×	×	√

mechanisms can be differentiated by measuring the potassium current before and after an action potential and measuring the potassium current at different voltage clamp levels. They can also be separated by applying different antagonists. Experiments such as these have not been reported.

B. Adaptation and binaural sluggishness

The adaptation mechanism included in this model might be hypothesized to affect sound localization ability, especially the localization of a moving sound source, to emphasize changes in the acoustic environment. It has been shown both empirically and in simulation that the dynamic IPD functions are sharper than the static functions. Provided that the response rate of an ensemble of IC neurons is an indication of a sound source in the azimuthal plane (Yin, 1994), the localization of a sound source moving within a given range in azimuth should be perceived moving in a wider range, if the rate of movement is high enough. It was found in psychophysics that when a sound motion was too fast to be followed, a ''wider'' or ''more diffused'' image was perceived (Grantham and Wightman, 1978). This finding is consistent with expectations from this model.

Psychophysical studies show that the auditory system responds sluggishly to changes in the interaural differences (Grantham and Wightman, 1978) and to the motion of a sound source (Blauert, 1972). Specifically, when a sound source moves rapidly, the motion can not be followed ''in detail.'' It is not clear whether the adaptation in the IC is related to the mechanism of binaural sluggishness. Psychoacoustic experiments (Grantham and Wightman, 1978) lead to estimates of frequency cutoff of the binaural system of about 10 Hz, corresponding to a time constant of about 16 ms, which is much shorter than the time constant of adaptation (500 ms) in the model. Thus the adaptation in the IC seems to be too slow to be responsible for binaural sluggishness.

A recent study by Joris (1996) explored the possible correlation between physiology and psychoacoustics related to binaural sluggishness. Interaural-correlation-modulated stimuli, similar to those used by Grantham (1982), were presented to anesthetized cats. Single-cell recordings were made from IC neurons. The function relating sensitivity to modulation, represented by the synchronization index versus the modulation frequency, shows a cut-off frequency near 50 Hz on average. The cutoff frequency is much higher than that measured psychophysically by Grantham and Wightman (1978), and indicates that sluggishness is probably due to mechanisms at higher levels in the auditory pathway.

C. Comparison with previous models

A trend in neural modeling is to include more physiological details in the models. The physiologically based models available so far that are most relevant to the model presented in this paper are the MSO model by Brughera *et al.* (1996) and the IC model by Cai *et al.* (1998). The difference between the IC model of Cai *et al.* (1998) and the IC model in this paper is that the current IC model incorporated an adaptation mechanism. The abilities of these three models are summarized in Table I.

The MSO model (Brughera *et al.*, 1996) can show unimodal ITD sensitivities in response to binaural tone stimuli and binaural beat stimuli. It can also show early or late inhibitions in response to binaural clicks.

In addition to properties demonstrated by the MSO model, the IC model without the adaptation mechanism (Cai *et al.*, 1998) shows bimodal IPD functions with some choices of the inhibitory parameters from the contralateral MSO. It may also show sensitivity to the direction and the speed of the binaural beat stimulus, when the contralateral inhibition lasts for a long time (tens of milliseconds). In response to pairs of binaural clicks, the model neuron showed ITD-dependent echo suppression. The responses of this model to depolarizing current injections show regular discharge patterns.

The IC model with the adaptation mechanism demonstrated sensitivities to dynamic temporal features not shown by the IC model without the AHP mechanism. These sensitivities are represented by the nonoverlapping IPD profiles in response to interaural phase-modulated stimuli, by a sharpened IPD function obtained from binaural beat stimulus, and by the changing response rate in the course of current injection. All of these features have been observed in physiological studies of the IC. The responses of the model to transient stimuli were not changed as compared with the Cai *et al.* (1998) model, since the adaptation mechanism had little effect if it was triggered infrequently.

Both of the IC models showed a decrease in phase locking to monaural stimuli as compared with the MSO model. In the current IC model, further decrease of phase locking was contributed by the adaptation mechanism; therefore the decrease in the synchronization index was more obvious.

However, the degree of phase locking was still high compared with physiological data.

In the current IC model, the excitatory inputs to the IC from ITD-sensitive neurons were responsible for the unimodal or sinusoid-like ITD functions of the IC. The inhibition to the MSO from onset cells was the cause of early inhibition observed in the IC model neuron. The inhibition to the IC from ITD-sensitive neurons was important for the behavior of the model that distinguished the IC from MSO, such as the bimodal ITD functions, ITD-dependent echo suppression, and direction and/or rate sensitivities. This inhibition was also the source of late inhibition in the simulation of the responses to binaural clicks. The adaptation mechanism was important for producing adaptive discharge patterns and sharpened dynamic IPD functions.

Alternative structures of models for the IC exist and could be evaluated. For example, an IC model which receives excitatory input from an ITD-sensitive neuron and inhibitory input from a monaural neuron should be able to describe unimodal ITD functions, early inhibition and late inhibition. If it has an adaptation mechanism, it will also describe adaptive discharge patterns and sharpened ITD functions. It will not explain the ITD-dependent echo suppression, the direction/rate sensitivities, and bimodal IPD functions. A MSO model with inhibition and an adaptation mechanism would show the same properties as this alternative IC model, including unimodal ITD function, early and/or late inhibition, adapting discharge patterns, and sharpened ITD functions.

D. Tests of the model and model predictions

The current model can be modified to address the simplifying assumption of the relay at DNLL. With a better understanding of the responses of the DNLL neuron, a model of the DNLL could be built and incorporated as an input to the IC model. It is expected that such a model would simulate more properties of the IC, such as the strong onset inhibition.

The mechanisms of the model could be tested with several types of physiological experiments. The hypothetical mechanism for the adapting behavior following discharge of the IC neuron is afterhyperpolarization caused by a calcium-activated, voltage-independent potassium channel. It would be of interest to test this hypothesis by blocking the calcium influx. If the adaptation is not calcium dependent, other channels or mechanisms might be responsible.

In the current models, it is assumed that the early inhibition comes from monaural neurons. This assumption can be tested by applying a binaural click following a monaural click. The bimodal ITD functions and direction and/or rate sensitivities in the responses of the model are caused by the interaction of excitatory and inhibitory ITD-sensitive neurons. This mechanism can be tested by blocking the inhibitory inputs to the IC.

The model can be used to predict the results of physiological experiments. First, since the ITD-dependent echo suppression is presumably caused by the inhibition from binaural neurons, the recovery curve with a monaural leading click should fall between those of the strongest and weakest suppressions obtained with binaural leading clicks with varied ITDs, based on the fact that the monaural response rate of a binaural neuron falls within the range of the responses to its bad ITD and good ITD. Second, short binaural noise bursts with various durations on the order of a few milliseconds followed by binaural clicks at good ITDs could be presented at varied interstimulus delay. If these stimuli were presented to the neurons which show long-lasting ITD-dependent echo suppression and sustained responses to long-lasting stimuli, it is predicted that the recovery function for different noise burst durations would not differ, since the inhibition to the IC is presumed to be driven by the stimulus onset. Third, if long-duration binaural tone bursts (e.g., 50 ms in duration) followed by short binaural tone bursts (e.g., 5 ms) were presented to direction or rate-sensitive neurons, keeping the ITD of the lagging tone at a good ITD and varying the ITD of the leading tone, it is predicted that the responses to the lagging tone would depend on the ITD of the leading tone, due to the rate-dependent nature of the afterhyperpolarization adaptation mechanism.

IV. CONCLUSION

The incorporation of an adaptation mechanism made it possible for the model to simulate the sensitivity of IC neurons to dynamic temporal features such as modulation of interaural phase and the adapting discharge patterns in response to current injection. At the same time, this mechanism did not deteriorate the abilities of our previous IC model (Cai *et al.*, 1998) which does not include an adaptation mechanism.

In conclusion, models for IC neurons with simple structures are consistent with a large amount of physiological data. These models contribute to our understanding of several mechanisms involved in binaural processing. In order to show essentially all the observed properties of IC discharge patterns, a model requires ITD-sensitive excitatory input, ITD-sensitive inhibitory input, and an adaptation mechanism such as afterhyperpolarization.

ACKNOWLEDGMENTS

This work was supported by NIH Grant No. R01-DC00100 (H.S.C.) and NIH Grant No. R29-DC01641 (L.H.C.) from the National Institute of Deafness and other Communication Disorders, NIH.

Blatz, L. A., and Magleby, K. L. (**1986**). ''Single apamin-clocked Ca-activated K+ channels of small conductance in cultured rat skeletal muscle,'' Nature (London) **323**, 718–720.

Blauert, J. (**1972**). ''On the lag of lateralization caused by interaural time and intensity differences,'' Audiology **11**, 265–270.

Brughera, A. R., Stutman, E. R., Carney, L. H., and Colburn, H. S. (**1996**). ''A model with excitation and inhibition for cells in the medial superior olive,'' Aud. Neurosci. **2**, 219–233.

Cai, H. (**1997**). ''Models for the binaural response properties of inferior colliculus neurons,'' dissertation, Boston University.

Cai, H., Carney, L. H., and Colburn, H. S. (**1998**). ''A model for binaural response properties of inferior colliculus neurons: I. A model with interaural time difference sensitive excitatory and inhibitory inputs,'' J. Acoust. Soc. Am. **103**, 475–493.

Carney, L. H. (**1993**). ''A model for the responses of low-frequency auditory-nerve fibers in cat,'' J. Acoust. Soc. Am. **93**, 401–417.

Carney, L. H., and Yin, T. C. T. (**1989**). ''Responses of low-frequency cells in the inferior colliculus to interaural time differences of clicks: Excitatory and inhibitory components,'' J. Neurophysiol. **62**, 144–161.
Colburn, H. S., and Ibrahim, H. (**1993**). ''Modeling of precedence effect behavior in single neurons and in human listeners,'' J. Acoust. Soc. Am. **93**, 2293(A).
Feliciano, M., and Thompson, A. M. (**1995**). ''Descending auditory cortical projections to midbrain and brainstem auditory structures in the cat,'' Assoc. Res. Otolaryngol. Abstr. **18**, 163.
Fitzpatrick, D. C., Kuwada, S., Batra, R., and Trahiotis, C. (**1995**). ''Neural responses to simple simulated echoes in the auditory brain stem of the unanesthetized rabbit,'' J. Neurophysiol. **74**, 2469–2486.
Grantham, D. W. (**1982**). ''Detectability of time-varying interaural correlation in narrow-band noise stimuli,'' J. Acoust. Soc. Am. **72**, 1178–1184.
Grantham, D. W., and Wightman, F. L. (**1978**). ''Detectability of varying interaural temporal differences,'' J. Acoust. Soc. Am. **63**, 511–523.
Hugues, M., Romey, G., Duval, D., Vincent, J. P., Lazdunski, M. (**1982**). ''Apamin as a selective blocker of the Ca-dependent K channel in neuroblastoma cells. Voltage-clamp and biochemical characterization,'' Proc. Natl. Acad. Sci. USA **79**, 1308–1312.
Joris, P. X. (**1996**). ''Brainstem responses to modulated interaural cues,'' Acustica **82**, Suppl.1, S97.
Kuwada, S., and Yin, T. C. T. (**1983**). ''Binaural interaction in low-frequency neurons in inferior colliculus of the cat. I. Effects of long interaural delays, intensity, and repetition rate on interaural delay function,'' J. Neurophysiol. **50**, 981–999.
Kuwada, S., Yin, T. C. T., Syka, J., Buunen, T. J. F., and Wickesberg, R. E. (**1984**). ''Binaural interaction in low-frequency neurons in inferior colliculus of the cat. IV. Comparison of monaural and binaural response properties,'' J. Neurophysiol. **51**, 1306–1325.
Litovsky R., and Yin, T. C. T. (**1993**). ''Single-unit responses to stimuli that mimic the precedence effect in the inferior colliculus of the cat,'' Assoc. Res. Otolaryngol. Abstr. **16**, 128.
Litovsky R., and Yin, T. C. T. (**1994**). ''Physiological correlates of the precedence effect: Free field recordings in the inferior colliculus of the cat,'' Assoc. Res. Otolaryngol. Abstr. **17**, 337.
Mardia, K. V. (**1972**). *Statistics of Directional Data* (Academic, London).
Mitani, A., Shimokouch, M., and Nomura, S. (**1983**). ''Effects of stimulation of the primary auditory cortex upon colliculogeniculate neurons in the inferior colliculus of the cat,'' Neurosci. Lett. **42**, 185–189.
Nelson, P. G., and Erulkar, S. D. (**1963**). ''Synaptic mechanisms of excitation and inhibition in the central auditory pathway,'' J. Neurophysiol. **26**, 908–923.
Oertel, D. (**1983**). ''Synaptic responses and electrical properties of cells in brain slices of the mouse anteroventral cochlear nucleus,'' J. Neurosci. **3**, 2043–2053.
Oliver, D. L., and Morest, D. K. (**1984**). ''The central nucleus of the inferior colliculus in the cat,'' J. Comp. Neurol. **222**, 237–264.
Oliver, D. L., Winer, J. A., Bechius, G. E., and Marie, R. L. S. (**1994**). ''Morphology of GABAergic neurons in the inferior colliculus of the cat,'' J. Comp. Neurol. **340**, 27–42.
Pennefather, P., Lancaster, B., Adams, P. R., and Nicoll, R. A. (**1985**). ''Two distinct Ca-dependent *K* currents in bullfrog sympthetic ganglion cells'' Proc. Natl. Acad. Sci. USA **83**, 3040–3044.
Peruzzi, D. (personal communication).
Peruzzi, D., and Oliver, D. L. (**1995**). ''Intrinsic membrane properties and morphology of neurons in the rat inferior colliculus,'' ARO, **18**, 515.
Romey, G., and Lazdunski, M. (**1984**). ''The coexistence in rat muscle cells of two distinct classes of Ca^{2+}-dependent K^+ channels with different pharmacological properties and different physiological functions,'' Biochem. Biophys. Res. Commun. **118**, 669–674.
Rothman, S. R., Young, E. D., and Manis, P. B. (**1993**). ''Convergence of auditory nerve fibers onto bushy cells in the ventral cochlear nucleus: implications of a computational model,'' J. Neurophysiol. **70**, 2562–2583.
Sah, P. (**1995**). ''Properties of channels mediating the apamin-insensitive afterhyperpolarization in vagal motoneurons,'' J. Neurophysiol. **74**, 1772–1776.
Sah, P., and Isaacson, J. S. (**1995**). ''Channels underlying the slow afterhyperpolarization in hippocampal pyramidal neurons: Neurotransmitters modulate the open probability,'' Neuron **15**, 435–441.
Shneiderman, A., Oliver, D. L., and Henkel, C. K. (**1988**). ''Connections of the dorsal nucleus of the lateral lemniscus: An inhibitory parallel pathway in the ascending auditory system?,'' J. Comp. Neurol. **276**, 188–208.
Spitzer, M. W., and Semple, M. N. (**1991**). ''Interaural phase coding in auditory midbrain: influence of dynamic stimulus features,'' Science **254**, 721–724.
Spitzer, M. W., and Semple, M. N. (**1993**). ''Responses of inferior colliculus neurons to time-varying interaural phase disparity: effects of shifting the locus of virtual motion,'' J. Neurophysiol. **69**, 1245–1263.
Sujaku, Y., Kuwada, S., and Yin, T. C. T. (**1981**). ''Binaural interaction in the cat inferior colliculus: comparison of the physiological data with a computer simulated model,'' in *Neuronal Mechanisms of Hearing*, edited by J. Syka and L. Aitkin (Plenum, New York), pp. 233–238.
Sun, X., Jen, P. H. S., Sun, D., and Zhang, S. (**1989**). ''Corticofugal influences on the responses of bat inferior collicular neurons to sound stimulation,'' Brain Res. **495**, 1–8.
Wu, S. H., and Oertel, D. (**1984**). ''Intracellular injection with horseradish peroxidase of physiologically characterized stellate and bushy cells in slices of mouse anteroventral cochlear nucleus,'' J. Neurosci. **4**, 1577–1588.
Yamada, W. M., Koch, C., and Adams, P. R. (**1989**). ''Multiple channels and calcium dynamics,'' in *Methods in Neuronal Modeling—From Synapese to Networks*, edited by Christof Koch and Idan Segev (MIT, Cambridge), pp. 97–133.
Yin, T. C. T. (**1994**). ''Physiological correlates of the precedence effect and summing localization in the inferior colliculus of the cat,'' J. Neurosci. **14**, 5170–5186.
Yin, T. C. T., and Kuwada, S. (**1983a**). ''Binaural interaction in low-frequency neurons in inferior colliculus of the cat. II. Effects of changing rate and direction of interaural phase,'' J. Neurophysiol. **50**, 1000–1019.
Yin, T. C. T., and Kuwada, S. (**1983b**). ''Binaural interaction in low-frequency neurons in inferior colliculus of the cat. III. Effects of changing frequency,'' J. Neurophysiol. **50**, 1020–1042.